*Int. J. Multiphase Flow* Vol. 8, No. 1, pp. 11–20, 1982
Printed in Great Britain.

0301-9322/82/010011-10$03.00/0
Pergamon/Elsevier

# A REGIME MAP FOR DIRECT CONTACT CONDENSATION

C. K. CHAN
Jet Propulsion Laboratories, Pasadena, California, U.S.A.

C. K. B. LEE
R&D Associates, Marina del Rey, California, U.S.A.

(*Received* 6 *February* 1980; *in revised form* 3 *May* 1981)

**Abstract**—Direct-contact condensation is studied by injecting steam downward through a pipe and out of the submerged end into a pool of subcooled water. The motion of the steam/water interface is recorded by high-speed movies and systematically classified, based on the injection rate and the pool subcooling. The resulting regime map shows the existence of three main condensation modes as the injection rate is reduced: At a high rate of steam injection (>125 kg/m$^2$s) an oscillatory jet is observed. At a low rate of injection (<50 kg/m$^2$s) a phenomenon called "steam chugging," in which the pool water periodically enters the injection pipe, is observed. At intermediate injection rates an oscillatory bubble exists continuously at the pipe exit.

## 1. INTRODUCTION

The injection of a vapor into a subcooled liquid of the same substance is a common event in many industrial two-phase flow systems, such as condensers, boilers and nuclear reactor coolant systems. The behavior of the interface, which is governed by the transfer processes in the vapor and liquid regions near the interface, is of prime interest in these applications. Because these problems are complex, the use of theoretical techniques is usually bypassed in favor of the simpler and more direct experimental approaches. This paper presents the results of an experimental study of steam injection at very subsonic injection rates.

Previous work in the field emphasized the stable sonic steam jets. In a steam jet condition, the momentum of the vapor is high compared to the surrounding liquid flow. The mechanism governing the heat transfer and the interface shape and motion, then, is the vapor momentum and the pool subcooling, as has been proved by various investigators. Kerney *et al.* (1972) studied the jet length of the sonic jet in an experiment using a horizontal submerged injection. For a small range of pool temperatures (28–85°C) they were able to show that the jet length is proportional to the square root of the injection rate and inversely proportional to the subcooling. The jet length was correlated with the steam mass flux and predicted to within 11 per cent of their measured data. Later, Young *et al.* (1974) performed steam injection experiments in which a horizontally injected sonic steam jet condensed in a co-current coaxial flow of subcooled water. The objective was to study the heat transfer at the steam/water interface. A correlation was obtained between the Reynolds (Re) number, which depends on the interface velocity as determined from the Reynolds fluxes, and the Stanton (St) number.

Experiments with a vertical downward discharge of steam into a subcooled pool have also been reported. Stanford & Webster (1972) demonstrated an interdependence between the jet length and two parameters: the diameter of the injection pipe and the rate of injection. Greef (1975) studied the same problem using sodium vapor jets and steam jets. Both studies extended the injection rate to slightly subsonic ranges and recorded the oscillatory behavior of the subsonic jet. Recently, Cumo *et al.* (1978) were able to correlate the heat-transfer coefficient (at the interface of sonic jets) with pool subcooling, steam mass flow, and pipe diameter. Their measured heat transfer coefficients are on the order of $10^3$ kW/m$^2$s. This order of magnitude agrees with the coefficients measured by Kerney *et al.* and Young *et al.* for horizontal sonic jets.

Experiments of steam injection at substantially lower flow rates than those described above have also been reported. In earlier work, the authors of this paper performed experiments to study the behavior of the interface at injection rates ranging from ~1.0 kg/m$^2$s to 175 kg/m$^2$s (Chan & Lee 1978; Lee 1979). We proposed that the various condensation modes observed be classified by a simple condensation regime map, using the pool temperature as the ordinate and the injection rate as the abscissa. The rationale for using these parameters was that the injection rate provides a measure of the driving mechanism, whereas the pool subcooling represents the magnitude of the condensation rate.

Later, Marks & Andeen (1979) presented a similar regime map, which covered two regimes and a smaller range of injection rates (up to 40 kg/m$^2$s). However, they did not discuss the criteria for identifying the boundary of each condensation mode.

This paper presents a more thorough regime map than the map we previously proposed (Chan & Lee 1978). The characteristics of each of the condensation modes are discussed in detail; and some steam-chugging pressure pulses typical of each mode of chugging are illustrated.

## 2. EXPERIMENTAL APPARATUS AND PROCEDURE

The apparatus used for the steam injection experiment comprises a boiler, a superheater, a surge tank, and a hexagonal test chamber, interconnected with pipelines of varying diameters (figure 1). Specifications for the equipment, rate of steam flow, etc. are detailed in the appendix. Demineralized water is pumped into the boiler, which generates saturated steam. The steam then passes through a superheater and into a surge tank monitored with a pressure transducer and thermocouples. The steam flows from the surge tank through a quick-acting solenoid valve, into a plastic or steel pipe, and out of the submerged end of the pipe into the test chamber.

The test chamber consists of two hexagonal sections, one stacked on top of the other. Openings in every face of the hexagons are covered by a glass plate when high-speed motion pictures are recording the process or by a stainless steel plate when various measuring devices

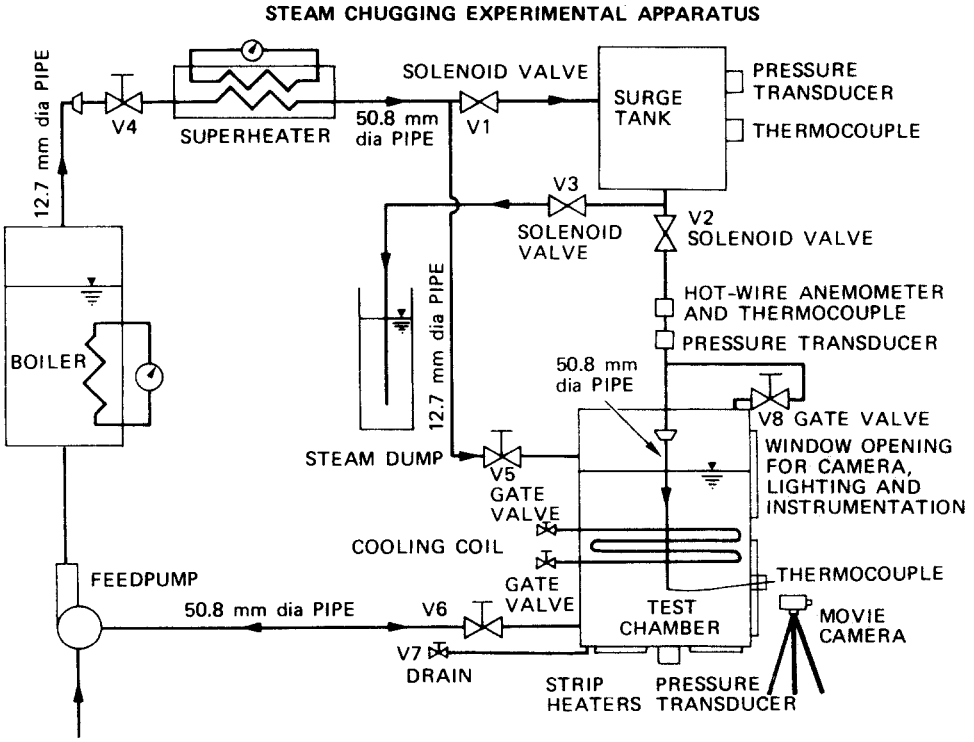


Figure 1. Experimental apparatus for steam chugging.

are to be inserted. A cooling coil is attached to the inner surface of the hexagon at the middle of the chamber. The bottom hexagon has two ports, one connecting the test chamber to a fresh-water supply line and one to a drain. As shown in figure 1, a line leads steam from the surge tank into the steam dump. Another line, with valve V5, is used for the degassing process. The line with valve V8 balances the pressure between the vent and the test chamber. All steam lines are wrapped with tape heaters and insulating materials to preclude condensatioon.

Before the test, the system is degassed in two stages. First, the air present in the system is purged with a steam flow. Second, the air dissolved in the distilled water of the system is reduced by heating the pool to ~80°C and recirculating the pool water for the generation of steam.

*Step I.* The air initially in the system is driven out by the steam generated in the boiler. This purging is initiated by turning on the boiler until the boiler pressure reaches the desired point. Then valves V4, V1 and V3 are opened, while valve V2 remains closed (figure 1). The air/steam mixture is discharged into the steam dump. Subsequently, valve V5 is opened so that the air in the pipe is driven into the test chamber atmosphere. Finally, the air in the vent pipe is driven into the pool by opening valve V2 and closing valves V3 and V5. To ensure the total purging of the air in the system, this process is normally continued for as much as an hour.

*Step II.* Opening valve V6 allows water to flow into the test chamber. The test chamber heater is turned on to purge the air initially dissolved in the water. Reabsorption of the air into the water is prevented by maintenance of a steady steam flow over the water surface through the line controlled by valve V5. Generally, the test chamber water is heated up to ~60°C, and then cooled by the cooling coil to the temperature desired for the particular experiment. The same water is used to generate the steam. At the end of the degassing process, valve V2 is closed so that no more steam is injected into the pool.

During the tests, the pool water level was 0.508 m and the end of the injection pipe submerged 0.254 m deep in the water. A Cr–Al thermocouple was installed at the vent exit. After the pool temperature reached the desired temperature, either by cooling with the cooling coil or heating with the bottom heaters, the surge tank was pressurized to the desired pressure and a quasi-steady stream of stream was then injected through the vent pipe into the pool by triggering valve V2. Simultaneously, the Hycam high-speed movie camera was also started to record the interface motion at the pipe exit. The steam flow rate was measured by two different methods, depending on the rate of flow. In the case of high injection rates (greater than 100 $kg/m^2s$) the steam mass fluxes were calculated from the pressure difference measured between the steam-supply and the ambient pressures. In the case of low steam-injection rates, the average steam mass fluxes were calculated from the total energy balance of the pool over a period of time.

## 3. RESULTS

### 3.1. *Observation of films*

It was observed from the high-speed films that the steam jet at sonic speed has a stable cone shape. However, when the flow is subsonic, the steam jet is unstable. This unstable jet persists until the steam mass flux is less than 150 $kg/m^2s$, when the shape of the steam region is an oscillatory bubble rather than an oscillatory cone. At even lower rates of steam flow, bubbles form intermittently and water rushes up the injection pipe periodically.

The interface behavior of the steam is not governed solely by the flow rate but is also affected by the pool temperature. For the range of flow rates under study, which was well below the sonic, the steam momentum was no longer important. When the pool temperature is low, the steam region normally exists well below the pipe exit as a cone or as a bubble with a diameter approximately equal to that of the injection pipe. However, at high pool temperatures the steam region tends to encapsulate part of the pipe above the vent.

### 3.2. *The condensation regime map*

These observations are illustrated with the flow regime map shown in figure 2, which is characterized by two parameters: the rate of vapor injection (steam mass flux) and the degree of liquid subcooling (pool temperature).

3.2.1. *Criteria for boundaries.* The boundaries of various condensation modes on the flow regime map are established by two criteria: (a) the location of the steam region relative to the pipe exit and (b) the location at which steam bubbles detach from the source. The horizontal boundary labeled *A–B* in figure 2 shows whether the steam region is completely below the pipe exit or has expanded to encapsulate part of the pipe. The vertical boundaries indicate how steam is being released from the pipe exit.

At low pool temperature and high steam mass flux (region 4), the bubbles detach from the steam region at the tip of the cone, which is usually about two pipe diameters below the pipe exit. As the mass flux is reduced, the point of bubble detachment moves up to within one pipe diameter below the exit. This is where the bubble oscillation region begins. In region 5, the distance between the point of detachment and the vent pipe is so small that the steam region assumes the shape of a spherical bubble. This distance marks the boundary between regions 4 and 5.

An even lower steam mass flux produces a detachment point closer to the vent exit and causes the water to surge up into the pipe periodically. This condition marks the boundaries between regions 5 and 6, the steam chugging region. For a given mass flow rate the steam region grows to encapsulate the vent pipe at high pool temperatures, and the point of detachment could be above the vent exit. The detached bubble floats up toward the pool surface while condensing.

Owing to the crude methods used in estimating the steam mass flux, the indicated locations of the boundaries of the condensation regimes are only approximate. However, these regimes illustrate the existence of the various characteristic interface motion patterns for different ranges of pool temperature and steam mass flux. Details of each condensation regime are discussed in the next section.

3.2.2. *Interface behavior in each regime.* The condensation regime map shown in figure 2 is derived for mass fluxes of 175 kg/m$^2$s to 1 kg/m$^2$s and pool temperatures of 40°C to 90°C. The vent pipe diameter is 0.051 m; the equivalent diameter of the hexagonal pool is 0.48 m. The pool pressure is atmospheric.

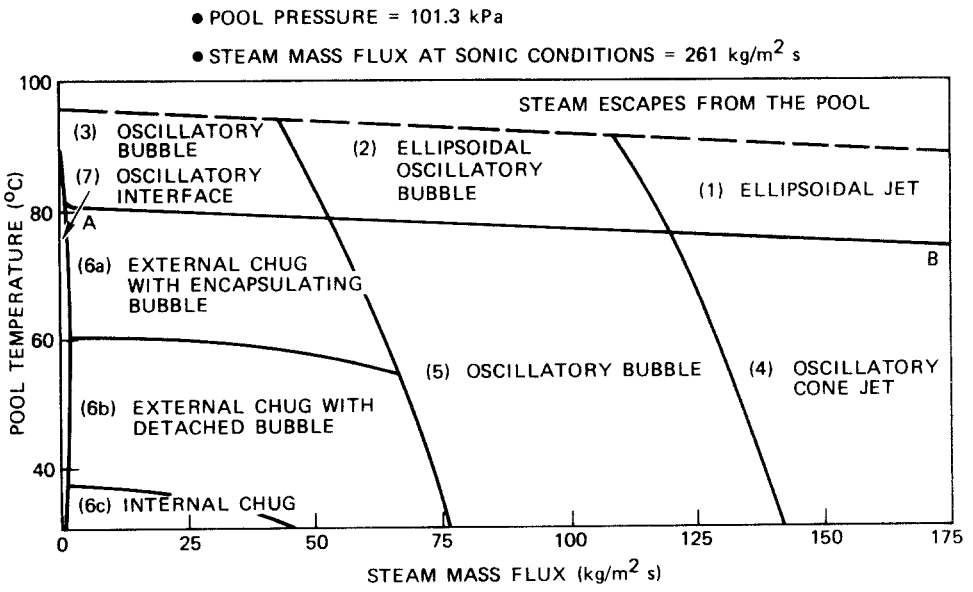


Figure 2. The condensation regime map.

At the high pool temperatures and high steam mass fluxes of region 1, the steam region existed as an ellipsoid that encapsulated the vent pipe. The small diameter of the ellipsoid was approximately eight vent diameters. No bubble detachment was observed in this region.

At the lower steam mass fluxes of region 2, the steam region still resembled an ellipsoid. However, an obvious bubble-detachment phenomenon could be identified (see figure 3). Detachment began approximately one pipe diameter below the pipe exit. When the steam region achieved an ellipsoidal shape, the liquid then started to penetrate the steam region and eventually separated the lower portion of the steam from the main steam region. The lower portion condensed as the upper portion grew to the ellipsoidal shape and the process repeated. The frequency of the detachment was about 11 Hz.

At the even lower mass fluxes of region 3, the steam region moved up to encapsulate more of the vent pipe, as shown in figure 4. Detachment occurred above the vent exit. The detachment process initially started as a liquid "belt" around the cylindrical bubble. As the belt tightened, the steam region above it was separated from the steam region below. The separated volume of steam condensed as it floated up toward the pool surface. The lower steam region, which remained encapsulating the pipe exit, then began to grow into another cylindrical column, another belt formed, and the process repeated. The detachment frequency was about 7 Hz.

In the low pool temperature and high mass fluxes of region 4, the steam region existed as an oscillatory conical jet below the vent exit (figure 5). The detachment point was about 1-1/2 pipe diameters below the vent exit. The bubble detachment process began as a liquid belt wrapped around the cone. As it began to tighten into the cone of steam, the cone was translating downward. Eventually, when detachment occurred, the cone had already moved approximately half a pipe diameter's distance. This process may also be described as an interface instability that grew as the steam region moved away from the vent exit until eventually the instability grew large enough that a volume of steam was cut off from the cone. The frequency of detachment was around 40 Hz.

At lower steam mass fluxes, the initial position of the instability was closer to the pipe exit. Thus, the actual point at which detachment occurred moved up to within one pipe diameter below the exit, which caused a change in shape of the steam region (figure 6) from an

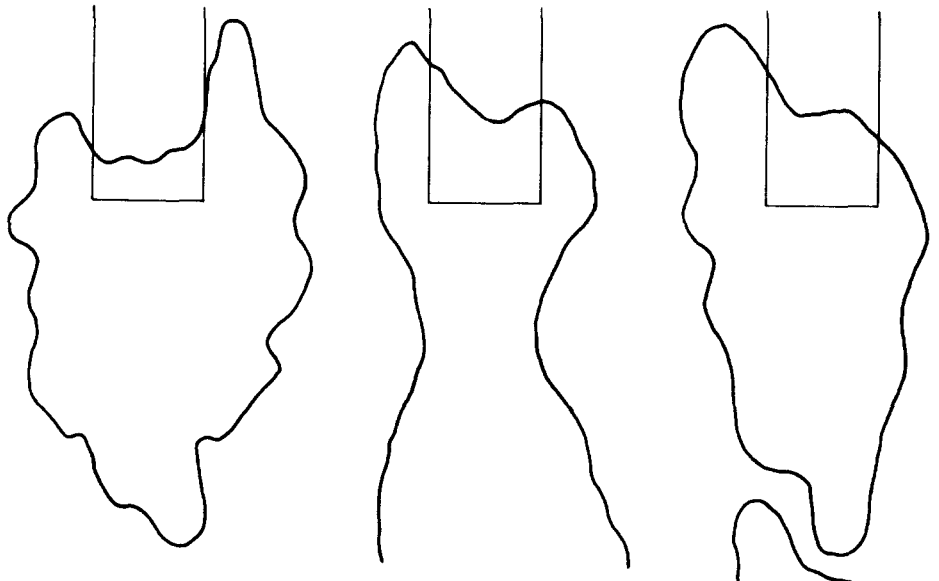


Figure 3. Ellipsoidal oscillatory bubble, region 2.

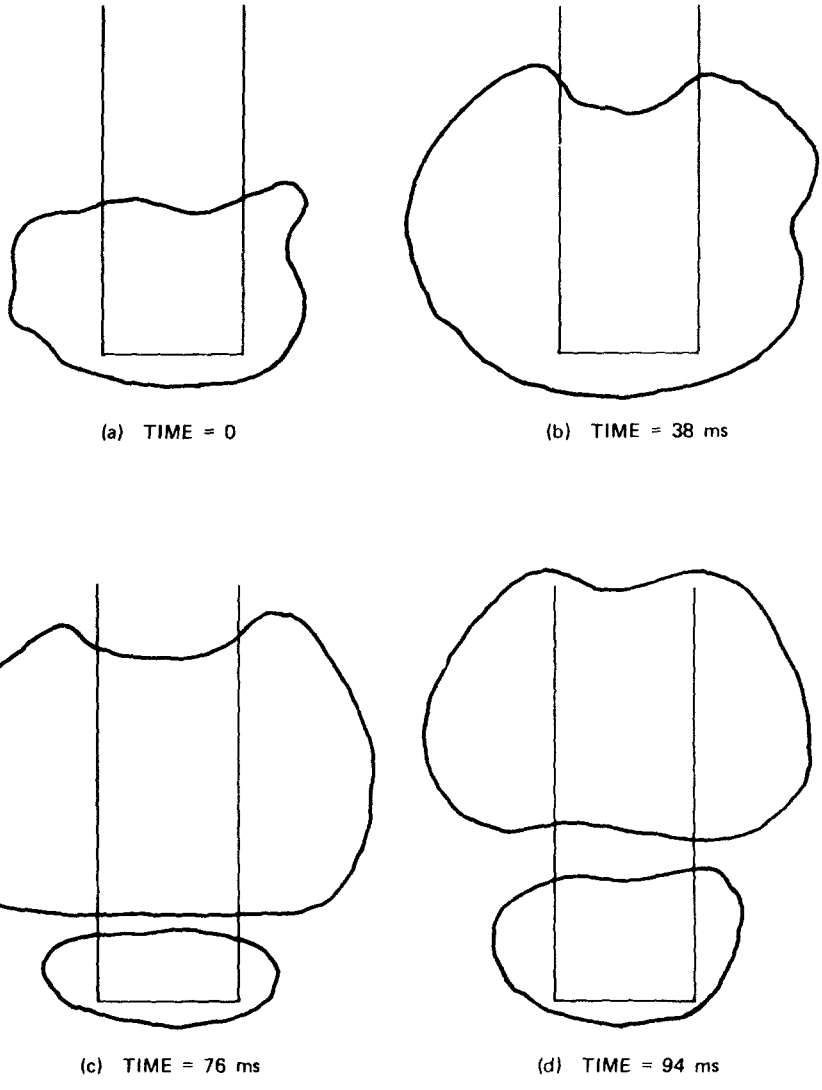


Figure 4. Oscillatory bubble, region 3.

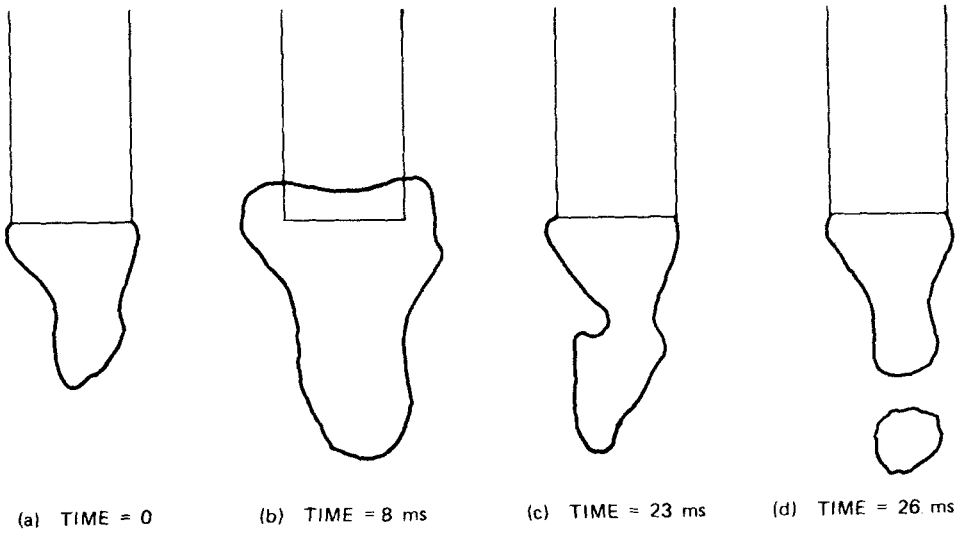


Figure 5. Oscillatory cone jet, region 4.

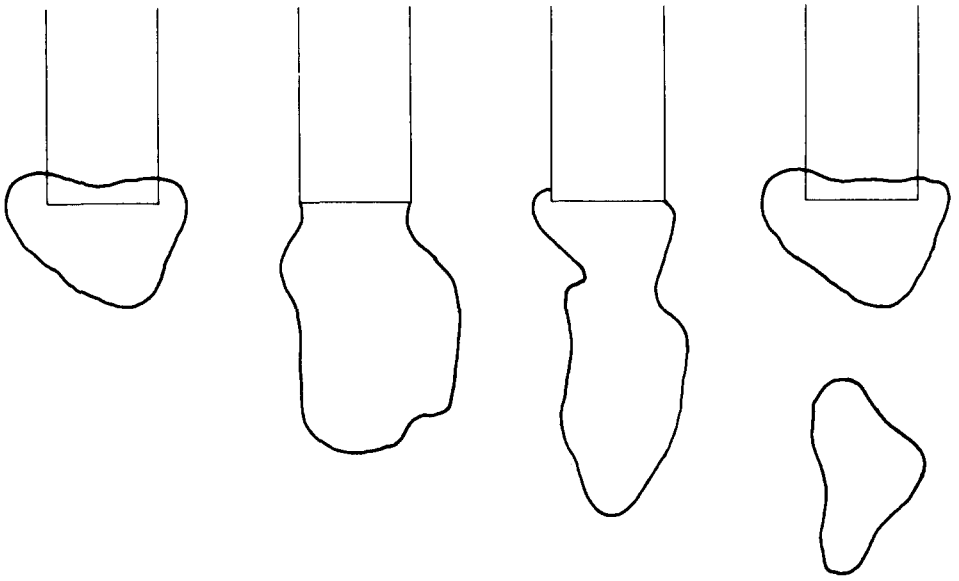


Figure 6. Oscillatory bubble, region 5.

oscillatory cone to one more closely resembling an oscillatory bubble. The frequency of bubble detachment was about 26 Hz.

Further reduction in the steam mass flux caused the point of detachment to occur closer to the pipe exit and ultimately right at the exit. This was taken as the boundary for the steam chugging regime, because the vapor region could only exist periodically in the pool, and the pool water would periodically enter the pipe.

The chugging regime could be separated into three different regions with distinct characteristics. The main features in each of these regions will be presented in the next section along with some pressure measurements at the pool bottom (figure 2: regions 6a, 6b, 6c).

The last condensation regime, region 7, involved no detachment process, and the steam/water interface existed right at the pipe exit. The steam mass flux was very low in this regime; in fact, in the present experiment the flow was so low that it was impossible to determine the steam mass flux. This condensation regime was characterized by an oscillatory interface at the pipe exit. The oscillations were just enough to induce convective processes in the water to transfer the heat from the condensation process at the interface to the pool.

Finally, for pool temperatures above the dashed line at the top of figure 2, steam was observed to escape from the pool surface.

### 3.3. *Steam chugging regimes*

With pool temperature low (below 80°C) and steam mass fluxes below about 75 kg/m$^2$s, water began to enter the vent pipe periodically. Unlike the case of a subsonic jet whose condensation phenomenon was characterized by high frequency but low pressure oscillations, the steam chugging phenomenon was characterized by pressure spikes of low frequency but large amplitude.

When the pool was cooled below approximately 40°C, it was observed that essentially all the condensation occurred inside the pipe. Therefore, this type of chugging is called "internal chugging". Bubble formation at the pipe exit was a rare event.

The interface motion inside the pipe for a typical chug is presented in figure 7. It was observed that as the water slug progressed downward toward the pipe exit, an annular flow developed; the steam region was surrounded by a layer of liquid adhering to the pipe wall. As the steam progressed further toward the exit, a small interface instability began to develop.

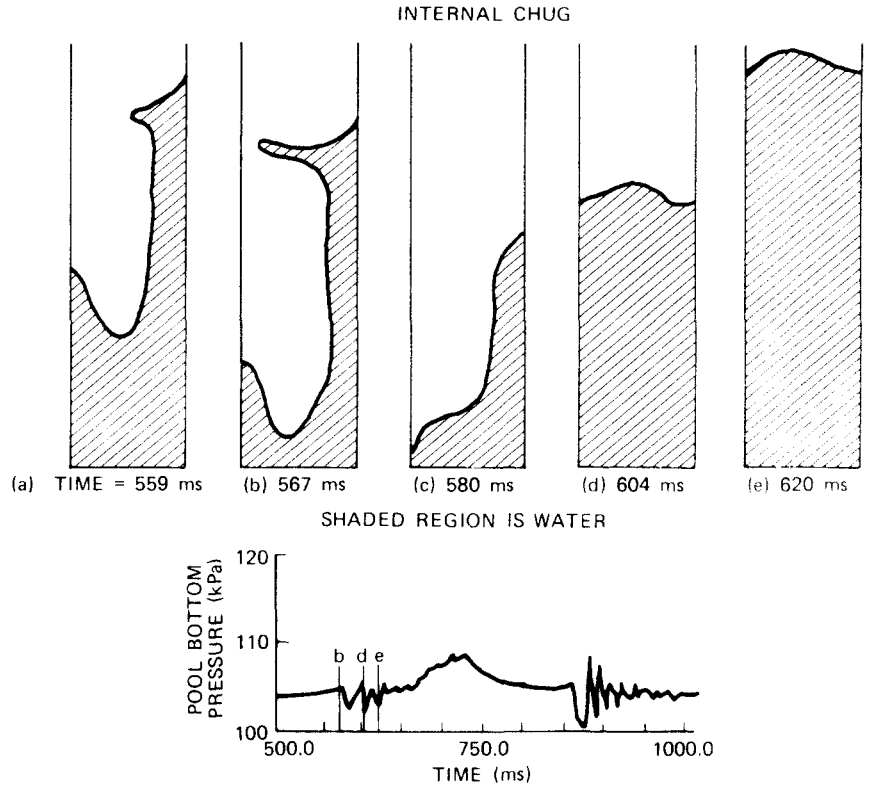


Figure 7. Internal chug, region 6c, at pool temperature of 44°C. Internal chug is infrequent at this temperature.

Eventually this interface instability became a small liquid jet that penetrated the steam region. When this liquid jet bridged the gap between the liquid layers on the pipe wall, a small volume of steam was isolated from the main stream. Immediately after the bridging phenomenon, the isolated volume of steam collapsed and water rushed back up the pipe.

Figure 7 also shows the corresponding pressure traces at the pool bottom. It is apparent that the internal changes did not lead to large pressure loads on the test section. The small oscillations in the pressure were due to the bubble collapse. The slow pressure increase after these oscillations corresponds to the time at which the water slug was rising up the pipe. Internal chugs usually occurred at the frequency of about 2–3 Hz.

At slightly higher pool temperatures (40–60°C) the interface progressed beyond the pipe exit, and a small cylindrical steam region formed there. However, immediately after the formation of the cylindrical bubble, the surrounding water rushed toward the steam region. This rush of water essentially cut off the cylindrical steam region from the pipe. Therefore, this type of chugging is referred to as an external chug with detached bubble (figure 8). After the detachment, the water rushed up the vent pipe. This type of chugging occurred at a frequency of about 2–3 Hz. Large negative and positive pressure spikes were recorded at the pool bottom.

Another type of chugging occurred more frequently at pool temperatures between 60°C and 80°C. This type involved the formation of a bubble after the interface progressed beyond the pipe exit. As the bubble grew, the steam region began to encapsulate the exit. This type is therefore called "external chugging with encapsulating bubble." The growth period followed the formation of a liquid belt around the lower part of the bubble. As the belt penetrated the bubble, a collapse began, while simultaneously the bubble was cut off from the pipe exit. The bottom pressure traces indicated some oscillations during the bubble growth period, a large negative spike during the collapse, and a short-duration but high-amplitude positive spike upon completion of the collapse.

A typical case of external chugging with encapsulating bubble is shown in figure 9. The

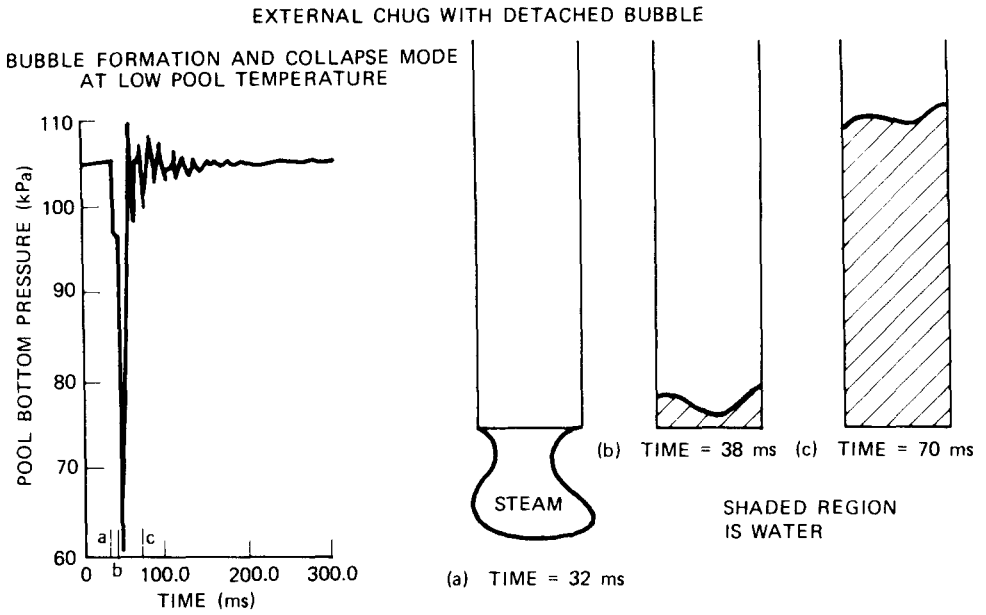


Figure 8. External chug with detached bubble region 6b, at pool temperature of 44°C. Detached bubble is most frequent at this temperature.

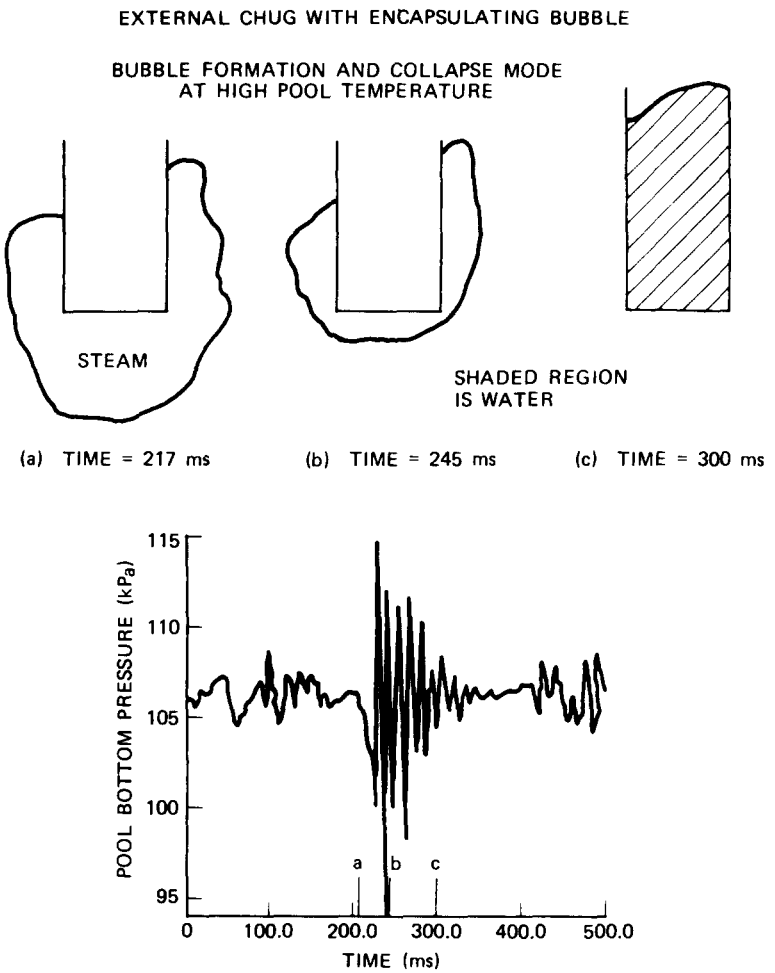


Figure 9. External chug with encapsulating bubble region 6a, at pool temperature of 62°C. Encapsulating bubble is most frequent at this temperature.

frequency for this type of chug was typically 1–2 Hz. The low frequency was due to the time taken for the bubble growth process.

These three types of chugging actually occur at every temperature range. However, the most frequent mode of chugging at low temperatures (below 40°C) is the internal chug; at midrange (40–60°C) is the detached bubble; and at high range (60–80°C) is the encapsulating bubble.

## 4. CONCLUSION

The rather complicated phenomena involved in steam injection can be systematically classified in terms of a simple condensation regime map. The coordinates of the map are the pool temperature, which characterizes the condensation, and the steam mass flux, which characterizes the driving mechanism. The classification is made by two simple criteria: the location of the steam region relative to the injection pipe exit and the position of the bubble detachment. Although this classification is based on a particular system geometry, it is expected that a steam injection system with a simple vent pipe would behave in a similar way.

The boundaries of the condensation regime map presented here are only approximate and are system dependent. Nonetheless, the map represents a step toward classifying complicated condensation modes commonly encountered in low-flow steam injection.

*Acknowledgements*—This work performed at the University of California Los Angeles, was supported in part by the U.S. Nuclear Regulatory Commission under Contract No. AT(48-24)-0342. C. K. B. Lee is grateful to R&D Associates for providing company time and resources to facilitate the writing of this paper, and to J. D. Radler for the expert editing.

## REFERENCES

CHAN, C. K., & LEE, C. K. B. 1978 Steam chugging in pressure suppression containment. Final Report submitted to the U.S. Nuclear Regulatory Commission, unpublished.

CUMO, M., FARELLO, G. E. & FERRARI, G. 1978 Heat transfer in condensing jets of steam in water. *Proc. 6th Int. Heat Transfer Conf.* Toronto **5**, 101–106.

GREEF, C. P. 1975 A study of the condensation of vapor jets injected into subcooled liquid pools, RD/B/N3262. Central Electricity Generating Board, Berkeley Nuclear Laboratories. United Kingdom.

KERNEY, P. J., FAETH, G. M. & OLSON, D. R. 1972 Penetration characteristics of a submerged steam jet. *A.I.Ch.E. J.* **18**(3), 548–553.

LEE, C. K. B. 1979 Hydrodynamical aspects of low flow vapor injection into subcooled water. Ph.D. dissertation, University of California, Los Angeles.

MARKS, J. S. & ANDEEN, G. B. 1979 Chugging and condensation oscillation. Presented at the *18th Natl. Heat Transfer Conf.*, San Diego, California, July.

STANFORD, L. E. & WEBSTER, C. C. 1972 Energy suppression and fission product transport in pressure-suppression pools. ORNL-TM-3448. Oak Ridge National Laboratory, Oak Ridge, Tennessee.

YOUNG, R. J., YANG, K. T. & NOVOTNY, J. L. 1974 Vapor–liquid interaction in a high velocity vapor jet condensing in a coaxial water flow. *J. Heat Transfer* **3**, 226–230.